Source identification in small spaces using field separation method: application to a car trunk

Alexandre Garcia, Yacine Braïkia, Christophe Langrenne, Eric Bavu, Manuel Melon

ACOUSTICS 2012

Source identification in small spaces using field separation method: application to a car trunk

A. Garcia, Y. Braikia, C. Langrenne, E. Bavu and M. Melon

Conservatoire National des Arts et Métiers, 292 rue Saint-Martin 75141 Paris Cedex 03
alexandre.garcia@cnam.fr

Acoustic holography is a powerful tool for the localization and ranking of sound sources. However, when dealing with non-anechoic spaces, classical methods have to be modified in order to take into account reflections on the testing room's walls and, if necessary, the field radiated by secondary sources. In this paper, the field separation method is used to overcome these problems. This method consists in measuring the acoustic pressure on a double layer half-sphere array which base is laying on the surface of interest. Then, by using spherical harmonic expansions, contributions from outgoing and incoming waves can be separated, if the impedance of the tested surface is high enough. Simulations on simple configurations and measurements on a car trunk mock-up are first presented. Measurements are performed using a double layer array made-up of 2×36 carefully calibrated microphones. Comparisons with results obtained with double layer SONAH are also shown. Finally, results obtained in a real car on a roller bench are reported.

1 Introduction

Identification of sound sources has received much attention among the scientific community over the last decades. Near-field Acoustic Holography (NAH) has proven to be a valuable measurement tool for the localization and ranking of sound sources. However, when measurements are performed in non anechoic and/or noisy spaces, results are no longer reliable. To overcome these problems several methods have been proposed. One can use reference microphones in order to separate contributions from incoherent sources. However, this technique requires an *a priori* knowledge of the locations of preponderant sources. Another solution consists in separating the contribution of the source of interest from the total field by using p-p or p-u probes arrays. For instance, Statistically Optimised Near-field Acoustical Holography (SONAH) has been rewritten for double layer pressure array [1] or single layer p-u probe array [2, 3]. Separation methods can also be used in spherical coordinates to recover free field conditions [4, 5, 6].
In this paper, separation techniques are used to characterize acoustic sources inside a car trunk, which has a rather small volume (about 0.5 m^2). Two methods are investigated: double layer pressure SONAH and spherical Field Separation Method (FSM). Several tests are performed: simulations are processed in a rectangular rigid room and measurements are conducted in a car trunk mock-up (with controlled sources) and in a real car trunk of a Peugeot 508 running on a roller bench.

2 Theory

2.1 Double layer SONAH

As the complete description of double layer pressure SONAH is given in Ref. [1], a brief overview will only be given here. The acoustic pressure is measured on two parallel planar arrays separated by a distance d, which should be smaller than the half-wavelength of the highest frequency of interest. With $d = 3$ cm, the maximum studied frequency f_c is equal to 5700 Hz. For double layer SONAH, two different sets of elementary plane waves are used to compute the acoustic field at a specific position. Each set corresponds to waves coming from a particular side of the array: the studied zone side or the room side. Making use of these functions allows the separation of acoustic fields coming from each side of the array. Several simulated and experimental results [1] showed that double layer SONAH was able to suppress the influence of secondary sources placed in the room side.

2.2 Field separation Method

The acoustic pressure is measured on two concentric hemispheres of radii a_1 and a_2. These two pressure fields are then expanded on normalized spherical harmonics. We suppose that the half-sphere base planes lay on a perfectly rigid surface. Thus, expansions can be performed on even spherical harmonics ($m + n$ is even) to respect the problem symmetry:

$$p(a_1,\theta,\phi) = \sum_{n=0}^{\infty}\sum_{m=-n}^{n} \alpha_{nm} Y_n^m(\theta,\phi) e^{j\omega t} \tag{1}$$

$$p(a_2,\theta,\phi) = \sum_{n=0}^{\infty}\sum_{m=-n}^{n} \beta_{nm} Y_n^m(\theta,\phi) e^{j\omega t} \tag{2}$$

where θ is the colatitude, ϕ is the longitude, and Y_{nm} are the normalized spherical harmonic functions. The α_{mn} and β_{mn} coefficients can be obtained from measurement data by matrix inversion or by expansion using orthonormal properties of Y_n^m. This formulation can be rewritten in terms of outgoing and standing waves:

$$\begin{aligned} p(a_1,\theta,\phi) &= \sum_{n=0}^{\infty}\sum_{m=-n}^{n} (a_{mn} h_n^{(2)}(ka_1) + b_{mn} j_n(ka_1)) Y_n^m(\theta,\phi) e^{j\omega t} \\ p(a_2,\theta,\phi) &= \sum_{n=0}^{\infty}\sum_{m=-n}^{n} (a_{mn} h_n^{(2)}(ka_2) + b_{mn} j_n(ka_2)) Y_n^m(\theta,\phi) e^{j\omega t} \end{aligned} \tag{3}$$

The spherical Bessel functions j_n represent the standing wave field while the spherical Hankel functions of second kind $h_n^{(2)}$ represent the outgoing field. The a_{mn} and b_{mn} coefficients are complex constants related to the measurement data and are the unknown quantities of the problem. Resolving this set of linear equations yields:

$$a_{mn} = \frac{j_n(ka_1)\beta_{mn} - j_n(ka_3)\alpha_{mn}}{\Delta}, \tag{4}$$

with: $\Delta = j_n(ka_1)h_n^{(2)}(ka_2) - j_n(ka_2)h_n^{(2)}(ka_1)$. The knowledge of the a_{mn} coefficients allows the calculation of the outgoing field. For performing expansions on even functions up to a maximum order $N = 7$, an array of at least $\sum_{i=0}^{N}(i+1) = 36$ probes is needed. When considering the external sphere of radius $a = 0.175$ m, the cut-off frequency is given by $f_c = \frac{cN}{2\pi a} \simeq 2180$ Hz.

2.3 Pros and cons

For SONAH, the separation of waves coming from each side of the array does not allow to remove sound coming from image sources included in the studied zone side. When dealing with large measurement rooms, image sources are generally farther away from the studied zone and does not

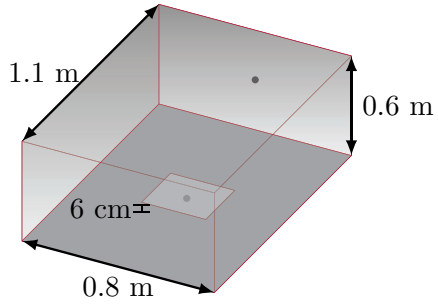

Figure 1: Geometry of the rigid rectangular room used for simulations. •: monopole locations. The square above one of the two monopoles shows the position of the array used for SONAH.

modify the calculated pressure. However, for small volumes like car trunks, image sources could lead to wrong results. On the contrary, FSM has the ability to remove all waves coming from outside the spherical array. As a consequence, this method should not be impacted by image sources. One drawback of hemispherical FSM is that the surface supporting the array should be rigid enough so that the duplication of the measurements (allowing spherical harmonic expansion) corresponds to the physical reality. Fortunately, many industrial sources are made of metal plates which can be, to a first approximation, assumed as perfectly reflective.

3 Simulations

The test chosen for the simulations uses very hard conditions: two monopoles are placed on the walls of a small rigid rectangular room. Dimensions of the room and positions of the monopoles are depicted in Figure 1. The array used for SONAH is made of $2 \times 6 \times 6$ microphones. The two measurement layers are separated from 2.5 cm, the first one is located at 6 cm of the ground and is centred on the monopole position. On each array, adjacent microphones are separated from 2.5 cm. Results are shown on Figure 2. The upper graph gives the pressure level (dB) at a point located near the center of the median plane of the array. One can see that the measured curve is ragged due to the modal behaviour of the tested room. After applying the SONAH algorithm, the curve is still ragged and does not agree well with the theoretical baffled monopole curve. A cumulative error rate between SONAH results and the baffled monopole response is calculated on 36 positions in the median plane. It is shown on the lower graph, with no surprise, that this index is high (> -10 dB). Due to the large number of undamped image sources in the studied zone side, double layer SONAH cannot give accurate results.

The same test is performed with FSM with the hemispherical array centred on the ground monopole. The array is made of 2×36 microphones distributed on two hemispheres having respective radii of 14.5 and 17.5 cm. Figure 3 shows the positions of the p-p probes. This distribution allows to obtain a small condition number (< 2) for $f < 2200$ Hz when inverting the matrix to process the α_{nm} and β_{nm} coefficients. Results are given in Figure 4 for a point located near the array's apex of the median half-sphere. The curve obtained using FSM is almost superposed to the baffled monopole curve

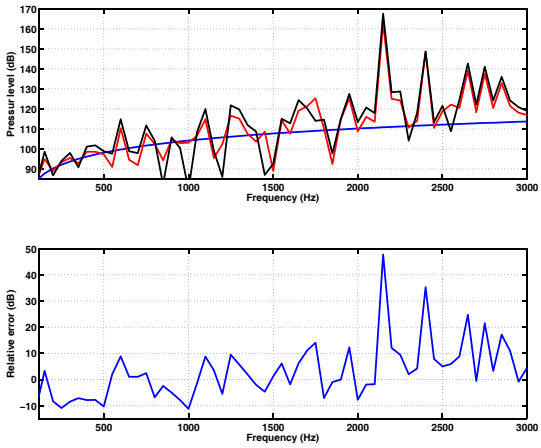

Figure 2: Upper graph: pressure level (dB) for a point located near the center of the median plane of the array . Black: measurement, red: SONAH processing and blue theoretical response of a baffled monopole.
Lower graph: relative error rate (dB) for SONAH on the 36 positions of the array.

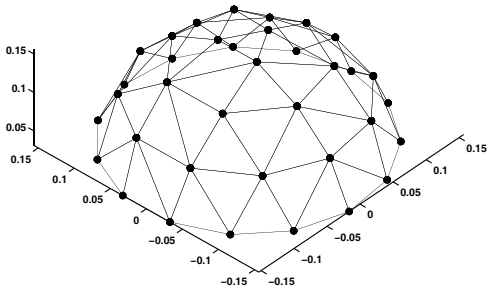

Figure 3: Geometry of the hemispherical array.

below 2200 Hz, which is the cut-off frequency of this particular array geometry. The cumulative error rate is rather small with a value varying between -40 to -17 dB in the baseband bandwidth. For this hard simulation configuration, FSM allowed recovering baffled source conditions. The next step consists in testing the two methods on real cases.

4 Measurements

In the presented measurements, two configurations have been tested: a car trunk mock-up with controlled sources and a real trunk of a Peugeot 508 car running on a roller bench.

4.1 Car trunk mock-up

The car trunk mock-up is made of 22 mm Medium Density Fiberboard wood. The chosen shape is a nearly rectangular cuboid of $1.1 \times 0.8 \times 0.6$ m^3 (one side deviate of about 10 degrees from verticality). Five 13 cm diameter Audax® HM130Z12 loudspeakers have been mounted on five of the

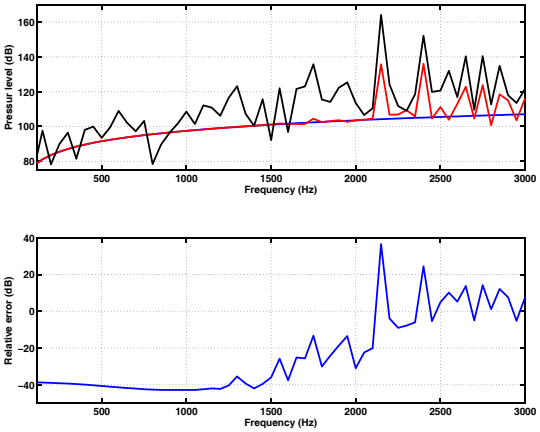

Figure 4: Upper graph: pressure level (dB) on the median half-sphere of the double layer array for a point located near the apex. Black: measurement, red: FSM processing and blue theoretical response of a baffled monopole. Lower graph: relative error rate (dB) for FSM on the 36 positions of the half-sphere.

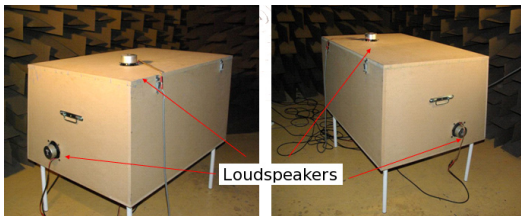

Figure 5: Outside views of the car trunk mock-up

six sides. A picture of the experimental set-up is given in Figure 5. For the measurements reported in this paper, three loudspeakers were driven by uncorrelated bandpass limited white noise signals.
For SONAH, the two microphone layers were separated from 3 cm. In each layer, the 36 microphones were distributed on a square grid with 6 cm steps. Results are reported on Figure 6 for a point located near the center of the array. The array is centred on the loudspeaker mounted in the bottom side of the mock-up. As already seen for the simulated case, double layer SONAH cannot remove all the reflections, thus giving a rugged frequency response. Nevertheless, some peaks, due to cavity resonances, are reduced.

When using FSM, we chose the same antenna geometry as in previously presented simulations. The antenna is also centred on the loudspeaker of interest. Results for a probe position near the apex of the median half-sphere are plotted in Figure 7. The frequency curve obtained using FSM processing is smoother than the measured one: reflections seem to be removed. Note that the steep slope around 1300 Hz can be found in the loudspeaker manufacturer documentation. A full scan of the cavity has also been performed. Figure 8 shows the measured pressure fields for 14 antenna locations. One can observe many high level zones which do not correspond to real source locations. After applying FSM algorithm (see Figure 9) the positions of two loudspeakers are recovered (note that the off-centred locations of maximum correspond to the real loudspeaker sites). The third loudspeaker located on the top-side is obviously not visible on the shown maps. In this experiment, FSM allows the removal of images sources and identifies the most vibrating surfaces.

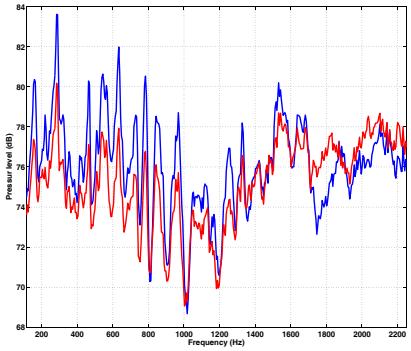

Figure 6: Pressure level (dB) on the median plane of the double layer array for a point located near the center. Blue: measurement, red: SONAH processing.

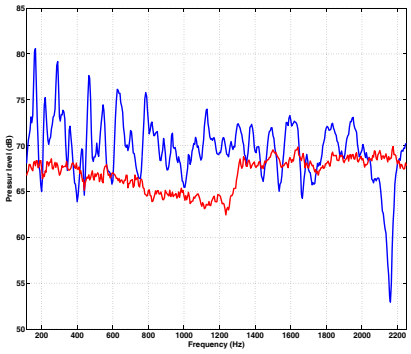

Figure 7: Pressure level (dB) on the median half-sphere of the double layer array in the 2000 Hz third octave for a point located near the center. Blue: measurement, red: FSM processing.

4.2 Car on a roller bench

FSM has also been tested on a real car: a Peugeot 508 SW on a roller bench (Figure 10). Figure 11 shows the antenna used for FSM in the trunk. The rollers are equipped with a high surface roughness material. The vehicle is running at a constant speed of 90 km/h under 3 conditions: engine off (neutral on), engine on with 3^{rd} or 5^{th} gear engaged.

Results at 125 Hz are shown in figure 12 for the 3 configurations tested. The three graphs nearly give the same results: at this speed and for a road with high roughness index, the rolling noise in the trunk is found to be predominant. Finally, the efficiency of two different mat materials has been tested. Results at 120 Hz are plotted on figures 13 and 14. One can see that the improved mat material can reduce radiated levels of more than 5 dB in the noisiest zones.

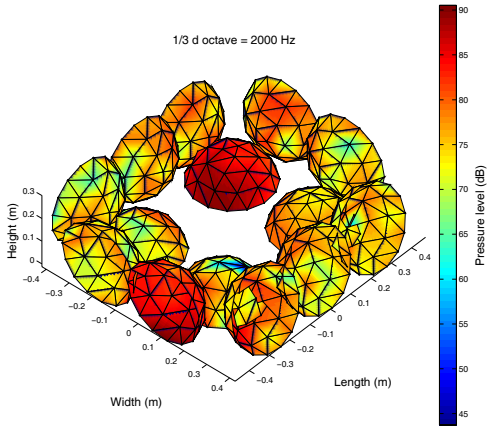

Figure 8: Measured pressure level (dB) on the median half-sphere of the double layer array in the 2000 Hz third octave band for 14 antenna locations.

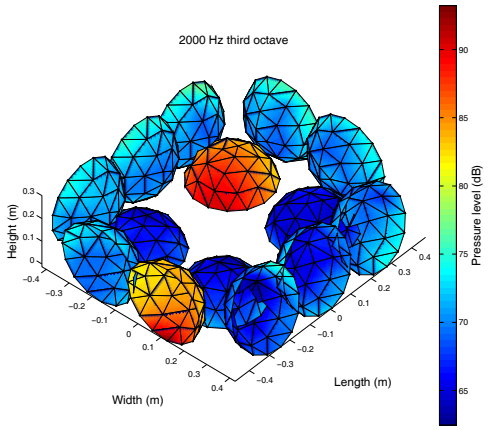

Figure 9: Pressure level (dB) on the median half-sphere of the double layer array after FSM processing in the 2000 Hz third octave band for 14 antenna locations.

Figure 10: Peugeot 508 on a roller bench.

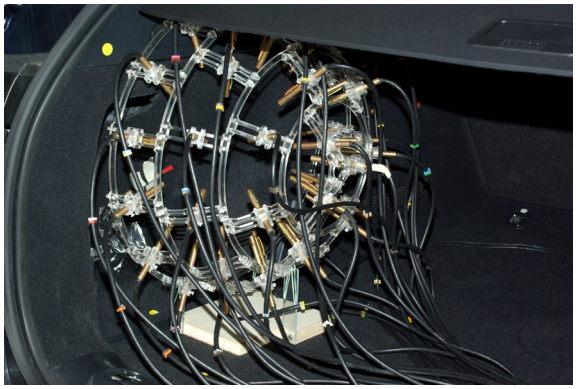

Figure 11: Hemispheric antenna in the 508 trunk.

5 Summary

In this paper, two separation methods, *i.e.*, double layer SONAH and FSM have been tested under highly confined conditions. For situations involving a large number of non negligible image sources, SONAH did not gave accurate results. This outcome can be explained by the fact that the separation is only performed between contributions coming from each side of the array. Thus, waves coming from image sources laying in the studied zone side are not subtracted. This drawback is not significant when performing measurements in large/damped rooms. On the other hand, when dealing with small volumes of about 1 m^3, this kind of separation is not sufficient.
FSM, which discriminates contributions coming from outside or inside the measurement sphere, is able to remove all image sources. Simulations and measurements performed here confirmed this point. However, one need to perform measurements with the antenna laying against a sufficiently rigid surface so that the pressure fields could be duplicated from half-spheres to spheres.

Acknowledgments

This work was carried out in the framework of the Licorve project with the financial support of the Fond Unique Interministériel (FUI). Measurements on the Peugeot 508 have been performed at Emitech CETRAM, Angoulême, France.

References

[1] J. Gomes, *Double Layer Microphone Array,* Master of Science in Engineering Thesis, University of Southern Denmark (2005).

[2] F. Jacobsen and V. Jaud, "Statistically optimized near field acoustic holography using an array of pressure-velocity probes", *J. Acoust. Soc. Am.* **121**(3), 1550–1558 (2007).

[3] Y.-B. Zhang, X.-Z. Chen, F. Jacobsen, "A sound field separation technique based on measurements with pressure-velocity probes", *J. Acoust. Soc. Am.* **125**(6), 3518–3521 (2009).

[4] G. Weinreich and E. B. Arnold, "Method for measuring acoustic radiation fields, *J. Acoust. Soc. Am.* **68**, 404–411 (1980).

[5] M. Melon, C. Langrenne, D. Rousseau, and P. Herzog, "Comparison of four subwoofer measurement techniques", *J. Audio. Eng. Soc.* **55**(12), 1077–91 (2007).

[6] M. Melon, C. Langrenne, P. Herzog, and A. Garcia, "Evaluation of a method for the measurement of subwoofers in usual rooms", *J. Acoust. Soc. Am.* **127**(1), 256–263 (2010).

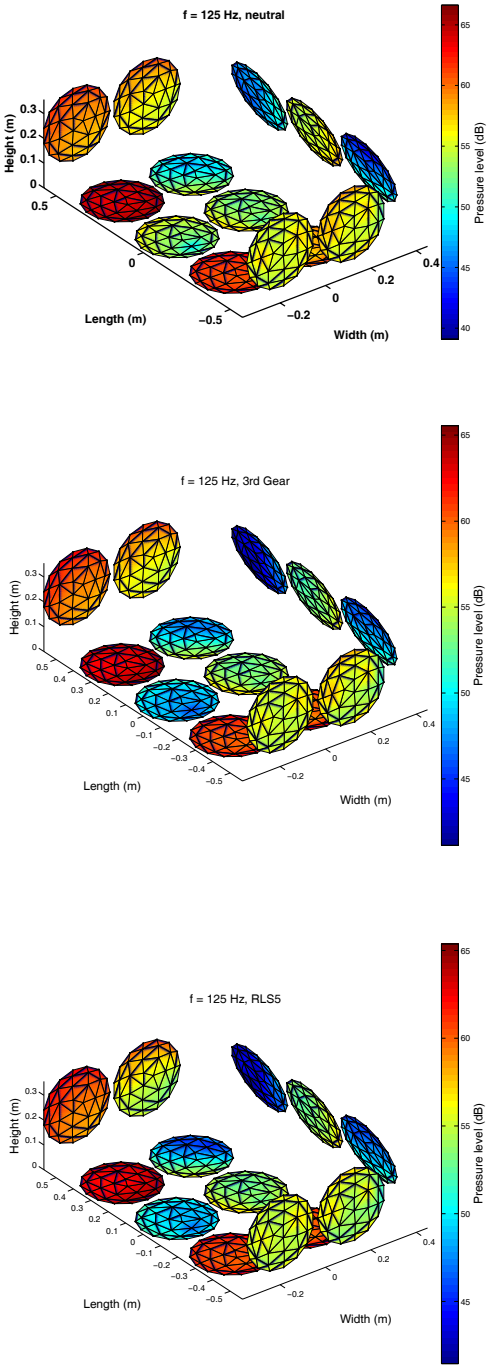

Figure 12: Scan of the trunk with vehicle running on a roller bench for 3 conditions: engine off (neutral on), engine on with 3^{rd} or 5^{th} gear engaged. Pressures are calculated on discs tangent to the apex of the array.

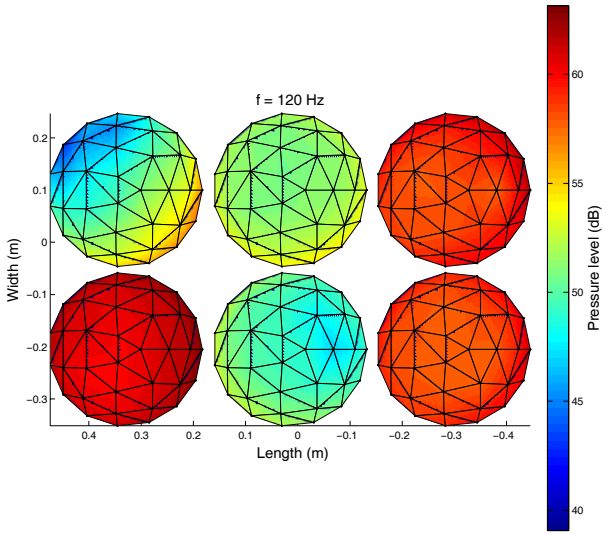

Figure 13: Scan of the trunk bottom at 120 Hz after FSM processing for a given mat material. Pressures are calculated on discs tangent to the apex of the array.

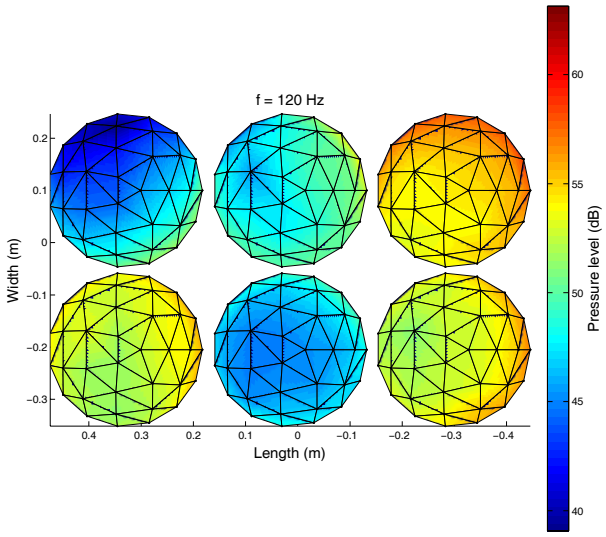

Figure 14: Scan of the trunk bottom at 120 Hz after FSM processing for an improved mat material. Pressures are calculated on discs tangent to the apex of the array.